LA-UR- 98-2689

Approved for public release; distribution is unlimited.

Title: Infrasonic Observation of Earthquakes

CONF-980779--

Author(s): Paul Mutschlecner
Rodney Whitaker

Submitted to: Forth International Workshop on Radar Polarimetry
July 13-17, 1998

MASTER

DISTRIBUTION OF THIS DOCUMENT IS UNLIMITED

Los Alamos
NATIONAL LABORATORY

Form 836 (10/96)

DISCLAIMER

J.P. MUTSCHLECNER--R. W. WHITAKER

Los Alamos National Laboratory
EES-8, MS-F659 Los Alamos, New Mexico 87545, USA
Ph: (505) 667-8063--Fax (505) 665-3415

ABSTRACT

Infrasound signals generated by earthquakes have been detected at arrays operated by the Los Alamos National Laboratory. Three modes of propagation are possible and all have been observed by us. The observations suggest that regions remote from the epicenters are excited and may serve as secondary source regions. A relation is found between the normalized peak amplitudes and the seismic magnitudes.

1 - INTRODUCTION.

Infrasound waves are propagated through the earth's atmosphere and, depending upon source and atmospheric conditions, may be detected at distances of hundreds to thousands of kilometers from the origin point. While there are several modes for propagation, the dominant one is ducting between the earth's surface and a stratospheric region at a height of about 50 kilometers. The frequency range of infrasound is from about 10^{-3} to about 10 Hz. Many natural sources and civilization sources of infrasound are known. Earthquakes are one of the most powerful sources of infrasound. It is presumable that strong vertical earth motion near the epicenter is responsible for generating most infrasonic signals. Several authors have reported on the detection of earthquake infrasound. The Los Alamos National Laboratory (LANL) has detected infrasound from a number of earthquakes and thus has been able to draw some general conclusions about these sources.

2 - MEASUREMENTS.

LANL operates several infrasound arrays; two have been particularly successful in detecting earthquake infrasound: one at Los Alamos, New Mexico, and one at St. George, Utah, U.S.A. The arrays consist of four infrasonic microphones in a triangular pattern with one central microphone; the typical spacing is 100 to 200 m. To reduce the effects of local wind turbulence noise a radial pattern of foam hoses are connected to each microphone giving collection of signal over a circular area of about 30 m diameter. The microphones are sensitive over the range of about 0.1 to 10 Hz. Data collection rates are typically 20 samples/s.

Data from an array are processed by a time-delay beamformer program which yields the quantities: signal amplitude, azimuth of arrival, trace velocity, average correlation across the array and peak frequency for each time interval. Trace velocity refers to the horizontal speed of passage of the signal waves across the array; it can be interpreted in terms of the inclination angle of the wave front to the vertical.

3 - EXAMPLES OF SIGNALS.

Figure 1 shows an example of the signal channel from the Northridge, California earthquake of 17 January, 1994 whose magnitude was $M_L = 6.4$. Four of the channels are shown so that the correlation can be seen. The signals are seen to be quite complex with a peak region but with many subsidiary features. The duration of earthquake signals may range from about one minute to over 30 minutes. Typical amplitudes are several microbars (1 microbar = 0.1 Pascal).

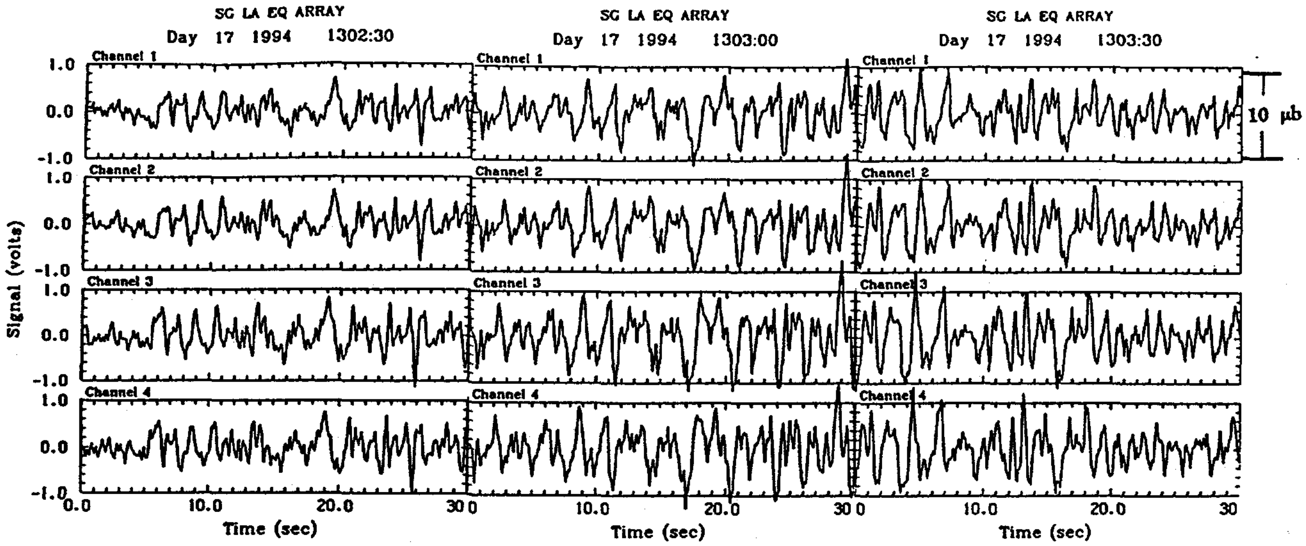

Figure 1. Four channels of data from the St. George array showing the primary signal region for the Northridge, California earthquake.

Figure 2 presents a summary of the beam-former analysis of the data for the same earthquake; each point represents the results of the analysis for a 20 second window. The top panel shows the azimuth of arrival (clockwise from 0^{o} at north). It is seen that the azimuths are variable before the signal and then tend to stabilize near a single azimuth which is very close to the great-circle azimuth to the earthquake epicenter. The next panel shows the trace velocity (m/s). Again, it is seen that during the signal period there is a strong concentration near a fixed value. The third panel shows the coefficient of correlation across the array. The correlation is low before the signals arrive and then reaches values near unity near the peak signal time. The bottom panel shows the average power per channel of the signals. Note especially for the last two panels that there are a number of distinct features related to the earthquake.

Figure 3 shows an example of the frequency content of an earthquake signal; in this case one near Socorro, New Mexico of magnitude $M_b = 4.6$. The time plot shows that the signal has strong energy between about 2.0 and 4.0 Hz. This is fairly typical for earthquake signals.

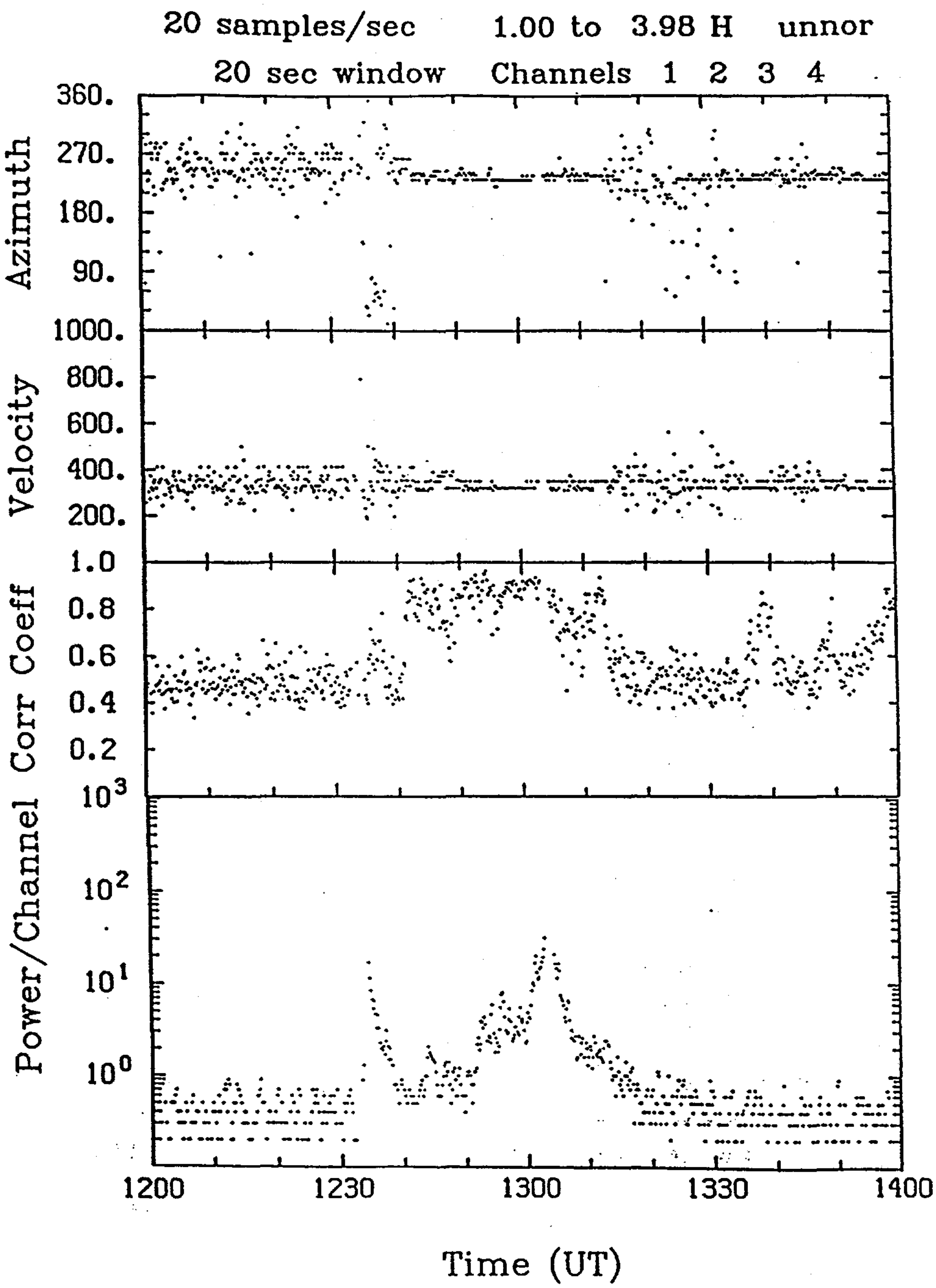

Figure 2. Results from the beamformer analysis of the Northridge earthquake data. Details are given in the text. The earthquake activity occurs roughly between 12:30 and 13:20 UT.

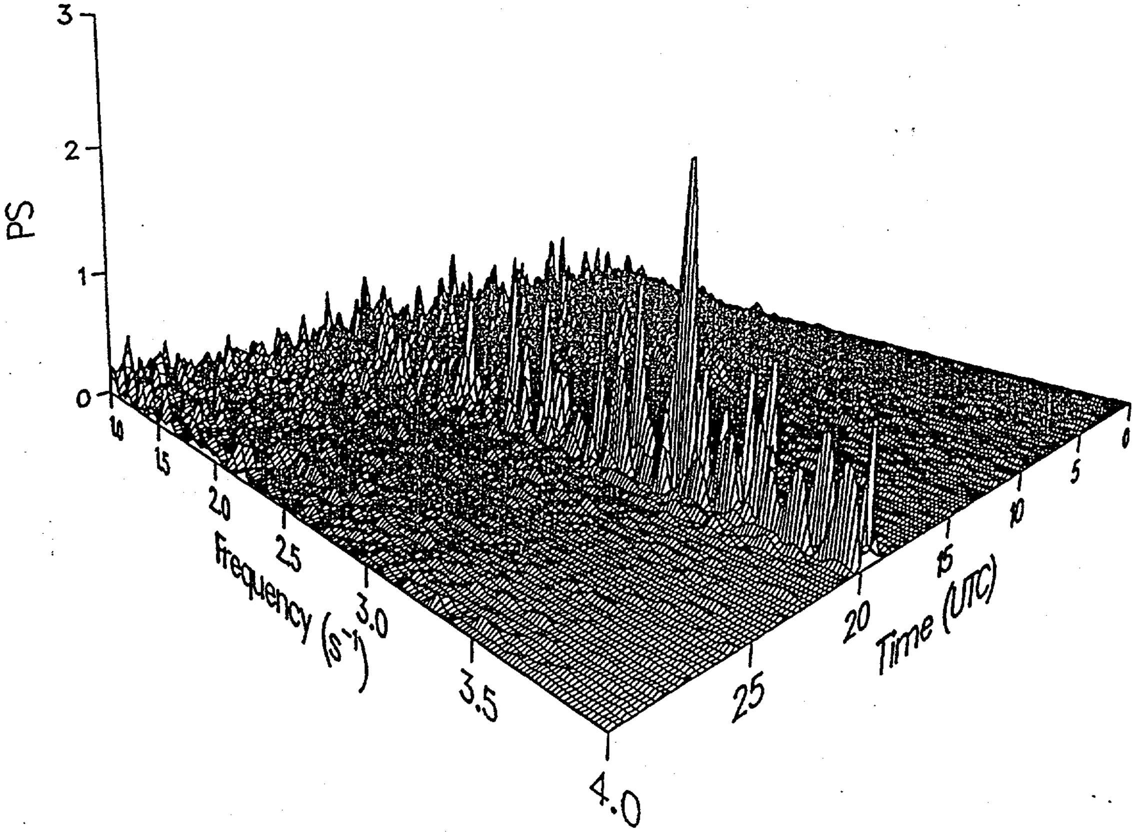

Figure 3. A time history plot of the power spectra for the Socorro, New Mexico earthquake.The earthquake activity is centered at about time marker minute 20.

4 - SIGNAL PROPAGATION.

In Fig. 4 we show the possible propagation paths for earthquake signals. In the first instance, infrasound waves may travel directly from the epicenter region through the atmosphere to the observer usually by the stratospheric ducting indicated earlier. A second possible path is for surface seismic waves, probably Rayleigh waves, to carry energy away from the epicenter to an outlying region where the energy is reradiated through earth motion which again generates infrasonic waves transmitted to the observer by atmospheric propagation. Finally, seismic waves may travel from the epicenter directly to the observer where the local ground motion is detected as infrasonic waves. In Fig. 2 the first power peak at about 12:35 UT is an example of this mode. All three types of propagation have been observed by us. Obviously the apparent or average speed of propagation from the epicenter to the observer will vary widely dependent upon the propagation path. A typical speed for pure acoustic transmission is about 290 m/s while direct seismic transmission may have speeds of about 3000 to 5000 m/s

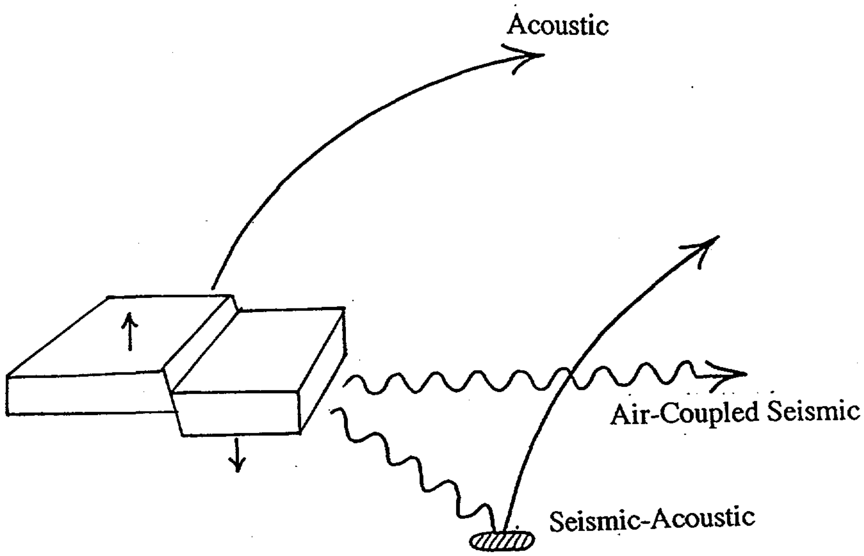

Figure 4. A schematic illustration of the three types of infrasonic propagation from an earthquake epicenter. See the text for a description.

5 - SECONDARY SOURCES.

As indicated earlier the duration of infrasonic signals from earthquakes may be substantial yet the duration of the ground motion near the epicenter is typically only a few seconds. We believe that this expansion of the signal duration is due primarily to the increase of the effective source region by the second type of transmission path just described, that is, the existence of secondary source regions which are established by surface waves from the epicenter. It can be seen that secondary source regions between the epicenter and the observer and those beyond the epicenter will, respectively, have shorter and longer transit times to the observer and hence lengthen the signal duration. In fact some events observed have distinctly separate peak regions corresponding to different secondary source regions. An example of this effect was seen in the signals from the Northridge earthquake. Figure 5 shows a possible interpretation of the signals in terms of secondary source regions. We have also seen a strong example of this effect in the Coalinga, California earthquake of 2 May, 1983 ($M_b = 6.2$) and arrays operated by the National Oceanographic and Atmospheric Administration detected strong secondary regions along the Rocky Mountain chain arising from the great earthquake in Alaska of 28 March, 1969 ($M_s = 7.0$).

It is likely that these effects can be seen only for larger earthquakes. Infrasonic observation of such secondary sources may be of value for better understanding of the remote effects of earthquakes, particularly where there is an absence of surface motion instrumentation.

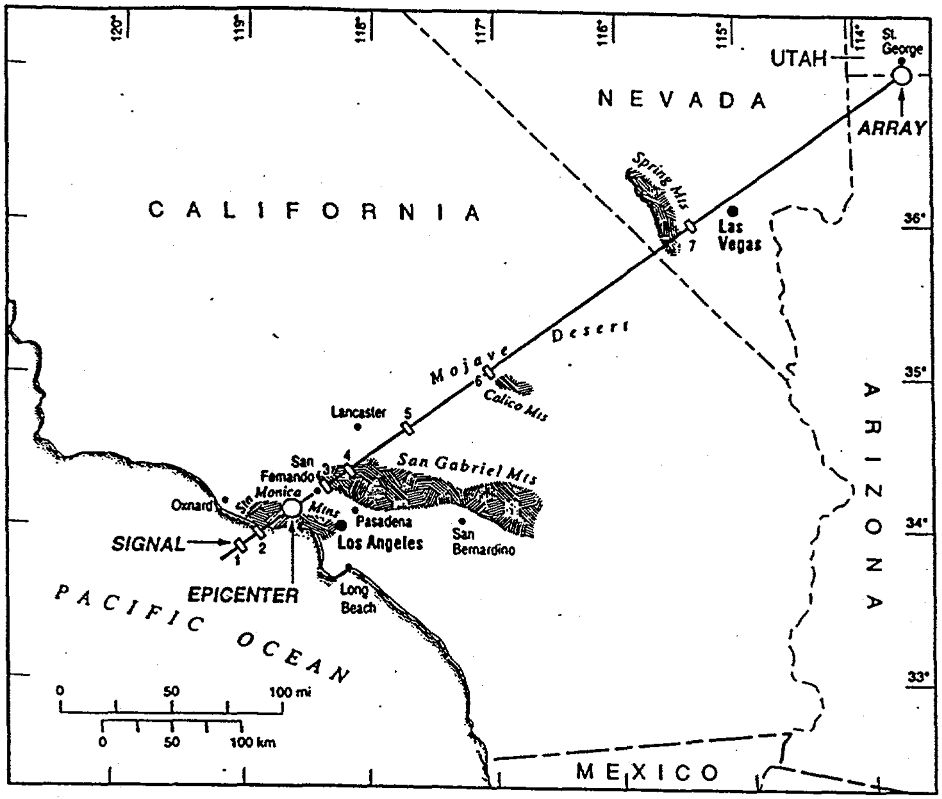

Figure 5. An interpretation of the signal sequence from the Northridge, California earthquake in terms of extended source regions. Seven separate regions are indentified along the path to the array location.

6 - MAGNITUDE-AMPLITUDE RELATION.

Observed infrasonic amplitudes are affected by the distance from the source by roughly a cylindrical falloff rate as a result of the ducting mentioned earlier. The amplitudes are also strongly affected by the stratospheric winds. This is because these winds play an essential role in the efficacy of the ducting. Thus when the stratospheric winds are in the direction of propagation there is strong ducting while counter winds produce poor ducting.. These two effects can be accounted for and the observed amplitudes, A_o, normalized to a "zero wind-standard distance" value, A_n, by the use of the following equation:

$$A_n = A_o \cdot \left(R / R_n\right)^s \cdot 10^{-kV} \qquad (1)$$

where R is the distance to the source, R_n is the normalized distance, and V is the component of the stratospheric wind at 50 km directed from the source to the observer. s and k are empirical constants which are here taken as 1.15 and 0.019 s/m respectively.

Using this normalization procedure all of our observations of peak amplitudes have been normalized; the standard distance used was 250 km. We have added one data point which is not ours from the Alaskan earthquake mentioned earlier since there is sparseness of data at very large magnitudes. Figure 6 shows the relation between the logarithm of the normalized amplitudes and the seismic magnitudes of most of the events which we have observed. Seismic magnitude is intrinsically a logarithmic scale, so that the resulting relation is

a log-log one. A least-squares line has been fitted to the data and it is seen that a linear fit is acceptable and that the scatter is small. In fact, it is somewhat surprising that the scatter is so small given the possible variation in the source conditions of earthquakes. It may be that there is a selection effect, in that, earthquakes that produce strong infrasound are of a particular class.

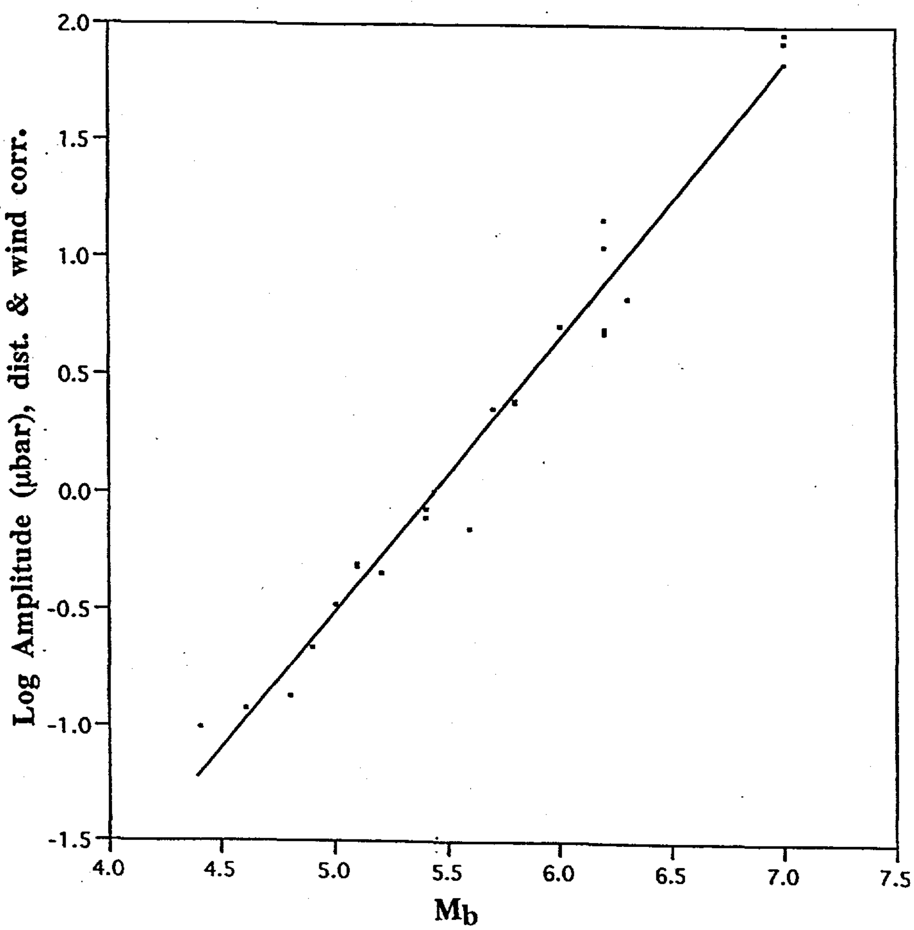

Figure 6. The relation between the peak amplitudes of infrasonic earthquake signals and the corresponding seismic magnitudes. The amplitudes have been normalized as described in the text.

7 - CONCLUSIONS.

Infrasonic observations of earthquakes provide a method of studying earthquakes and their effects on the ground motion of remote regions independent of the normal seismic measurement method. The amplitude-magnitude relation which we have determined gives the ability to estimate the infrasonic detectability of earthquakes. It is hoped that a study combining the infrasonic measurements with seismic source characteristics will allow a better understanding of the physical mechanism for the signal generation.